This project is funded by the European Union

AHEAD Workpackage 8
JRA X-ray optics

Deliverable D8.6 – D40

Screening Facility Technical Assembly Completion Report

Written by	Daniele Spiga (INAF/OAB)	
Checked by	Vadim Burwitz (MPE)	
Distribution List	AHEAD Management Team Vadim Burwitz WP8.0, WP8.1, WP8.3 Dick Willingale WP8.1 Rene Hudec WP8.1 Daniele Spiga WP8.1, WP8.2	
Distribution Date	Draft version	Jan 11, 2018
	Final version	Jan 18, 2018

1. STATUS OF THE PROJECT

Large X-ray facilities operating in high vacuum are required to efficiently test large aperture X-ray optical systems, or at least a significant sub-aperture. This poses a challenge for X-ray tests of optical X-ray assemblies based on a modular approach such as the ATHENA X-ray telescope.[1] ATHENA's optical system will have an outer diameter of 2.5-3 m, a 12 m focal length, an approx. 2 m^2 effective area at 1 keV, an angular resolution better than 5 arcsec HEW (*half-energy-width*) at 1 keV, and better than 10 arcsec at 6 keV.[2] In order to reach these performances, more than 1000 X-ray Mirror Modules (MMs) based on Silicon Pore Optics (SPO) have to be manufactured, tested, and qualified before the accurate alignment and integration into the supporting structure.[3] Each pore in each MM reproduces the Wolter-I (parabola+hyperbola) configuration and, owing to the wedged ribs, all the pores in an MM converge to focus.[4] Each MM integrated in ATHENA has to be accurately co-axially and co-focally aligned, but some alignment error is unavoidable. Hence, each individual, flight-grade MM has to be characterized by an angular resolution much better than 5 arcsec,[5][6] and only the most performing MMs out of the industrial production line can be selected to be integrated. Indeed, because of the small pore size (a few mm^2), metrological tests on the MM stacks are extremely difficult, and a reliable qualification test can be a direct measurement of the optical performances in X-rays. This also offers the possibility to reliably align the parabolic and the hyperbolic stack of the MM, as the maximization of the effective area - corresponding to the best align condition - can be checked at-wavelength. A measurement at PANTER would enable a true full-illumination test, but PANTER is a very large facility and cannot be routinely employed to perform the functional test of 1000 MMs. Finally, the testing facility cannot be moved near the MM production site, which imply a continuous module transportation across Europe.

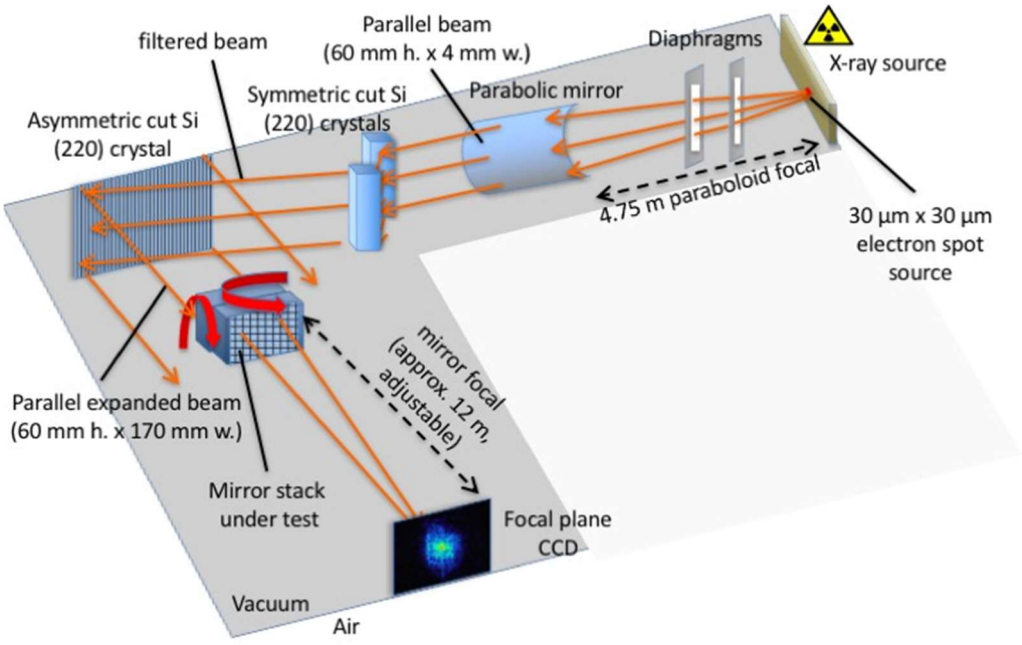

Fig. 1: schematic design of the BEaTriX facility in the 4.51 keV setup. The beam diverging from a microfocus X-ray source is collimated by a precisely figured paraboloidal mirror with the source in its focus. The beam has now a 4 mm (width) x 60 mm (height) size and the subsequent diffraction operated by a pair of symmetric silicon crystals precisely isolates the 4.51 keV fluorescence line. The horizontal expansion of the beam is operated by an asymmetrically-cut silicon crystal with respect to the (220) planes. The expanded beam (170 mm × 60 mm) can be used to illuminate the aperture of the focusing device under test, and the focus is directly observed by means of an imaging detector.

The solution we are developing as part of the present AHEAD project is a compact facility to generate a broad, parallel, uniform, monochromatic, and polarized X-ray beam, named BEaTriX[7] (*Beam Expander Testing X-ray facility*) to the specific end of testing ATHENA MMs in full illumination, with reduced costs and in a time short enough to sustain a production rate of 2-3 MM modules per day, and so return a prompt feedback to the manufacturer. BEaTriX[6][7][8] is being realized at INAF/OAB, to be possibly replicated at the industrial production site of the MMs. Specifications include:

i) an X-ray beam with minimum size of 120 mm x 60 mm to fully illuminate the largest apertures of MMs;
ii) very low residual divergence (< 1.5 arcsec HEW), aiming to reliably characterize MM PSFs (*point spread functions*) with an intrinsic HEW of 3-4 arcsec;
iii) high beam uniformity, to equally characterize the entire optical surface;
iv) monochromatic energy, selectable between 1.49 keV and 4.51 keV;
v) compact size to fit a small laboratory (7 m x 14 m), and reduce the test chamber evacuation time.

In the previous report, we had shown the updated project of BEaTriX. A schematic layout of the facility is described in Fig. 1, along with a short summary of the working principle. Here we report the advancement status of the project. Work is not complete yet, but is actively progressing on different fronts:

a) Simulation of the expected performances, with ideal/real components, in their nominal positions or slightly displaced, in order to freeze the manufacturing tolerances.
b) Technical design of the low-vacuum (10^{-2} mbar) system, including vacuum tubes, pumps, and motorized stages.
c) Procurement and manufacturing of the optical components (crystal, mirror, X-ray source).
d) Realization of the laboratory to host the X-ray facility.

2. PERFORMANCE SIMULATION AND ALIGNMENT TOLERANCES

A fundamental step in the facility realization and assembly is represented by the simulation of the BEaTriX system not only in the best align condition, but also in presence of manufacturing defects (e.g., the mirror surface) and misalignments. A detailed ray-tracing program has been developed at INAF-OAB to investigate the achievable performances (uniformity, intensity, collimation) of the expanded beam. The reference frame and the simulated components are shown in Fig. 2, some traced rays have been drawn in Fig. 3.

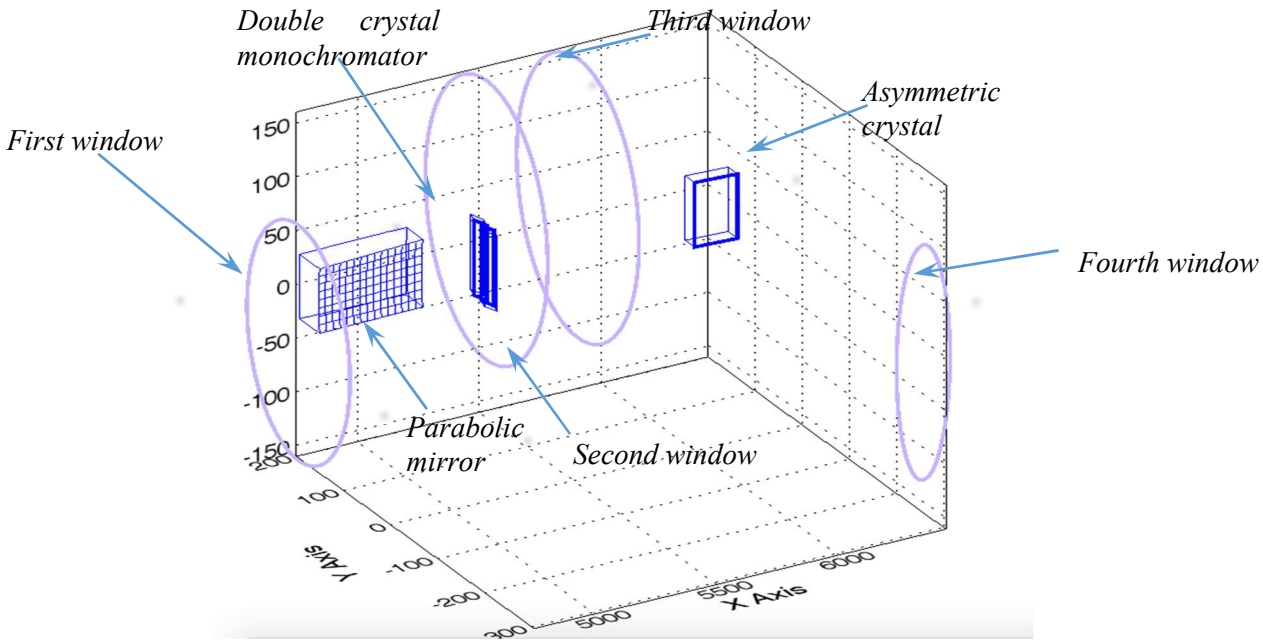

Fig. 2: the reference frame used for the present description of the BEaTriX facility. The z-axis is oriented vertically. We have simulated the incidence from the X-ray microfocus source (not visible, in the frame origin, on the left side) of a number of X-rays. We have included the mirror, the monochromator, the beam expander, and also the diaphragms connecting the vacuum chambers that might represent vignetting sources. Their positions were inferred from the vacuum system design (Sect. 3).

This project is funded by the European Union

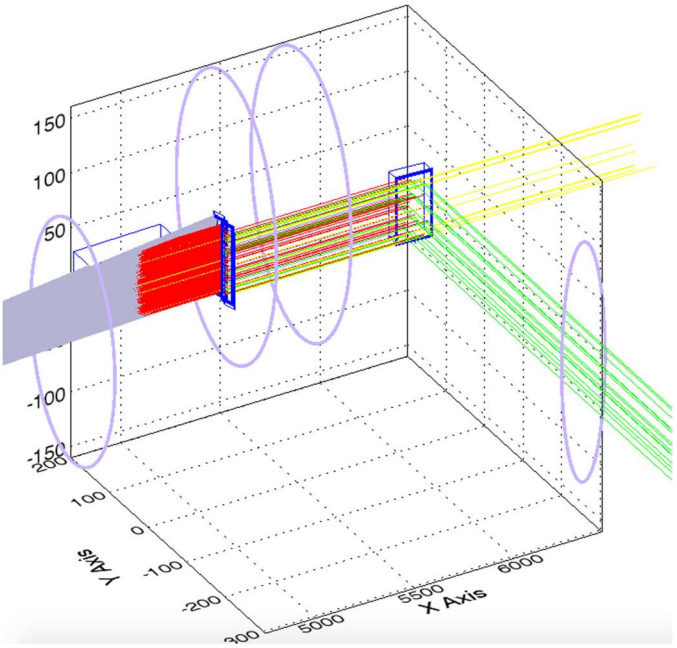

Fig. 3: simulated performance of the BEaTriX setup at 4.51 keV. The components and the circular diaphragms are shown in blue and purple. Launching 5000 rays from the source, they are labelled with colours depending on their fate. Red rays are absorbed in residual air or by the optical elements, grey rays are blocked, yellow rays have gone astray, orange rays are reflected in grazing incidence by the asymmetric crystal, and green rays are finally found in the expanded beam.

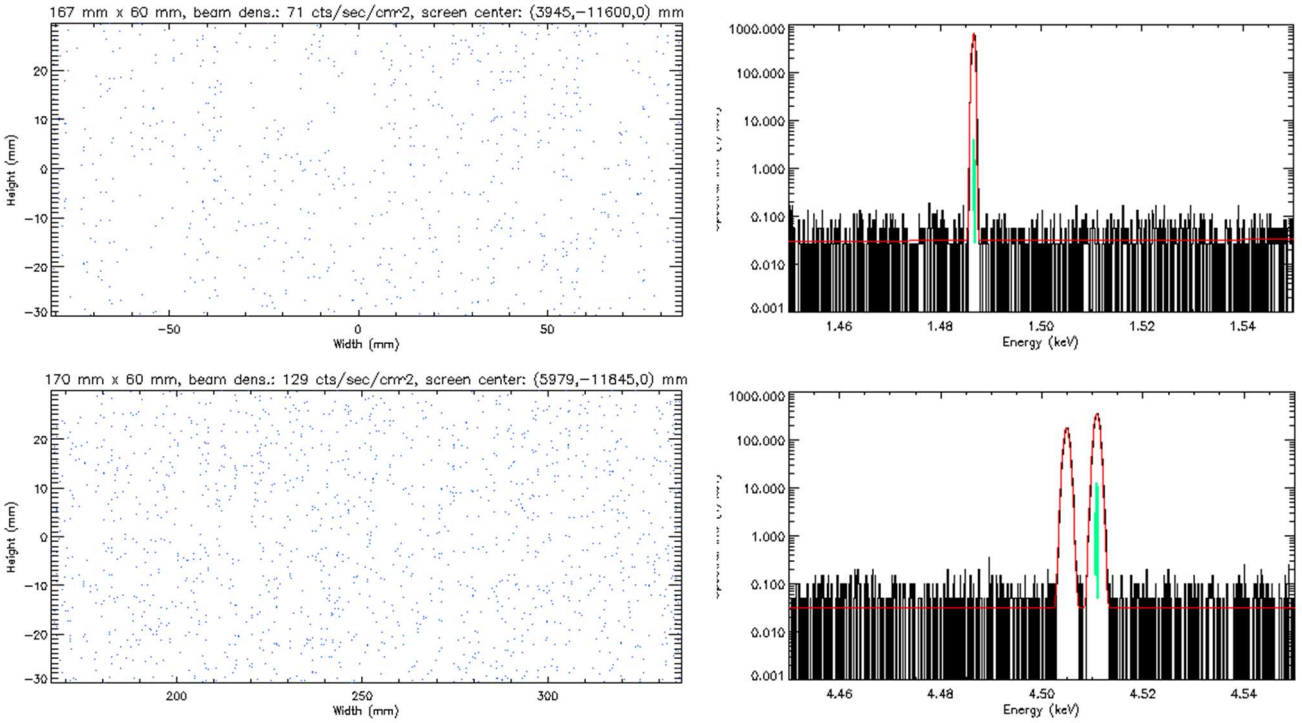

Fig. 4: simulated distribution at the focal plane (left, without SPO module) and filtered spectra (right) of the expanded beam at 1.49 keV (top) and 4.51 keV (bottom), after launching 500000 rays. The Al-Kα line is a close doublet, but only the Kα1 line is selected. The Ti-Kα doublet is, in contrast, well resolved.

Some results are displayed in Fig. 4: the detection plane, at a 12 m distance from the beam expanding crystal, is uniformly covered with a photon flux over a 170 x 60 mm rectangle, i.e., larger than required to illuminate the aperture of the largest SPO mirror modules. Accounting for the brilliance of a microfocus source, the predicted beam intensity is 70 counts/s/cm^2 at 1.49 keV and 130 counts/s/cm^2 at 4.51 keV, largely sufficient to characterize a SPO module in a few minutes.

When it comes to the beam collimation, the theoretical simulated performances are plotted in Fig. 5. The horizontal divergence is compressed within 0.1 arcsec, while the vertical divergence (which determines the angular dispersion in the incidence plane of the SPO under test) is near 1 arcsec FWHM. It is the source's vertical dimension and its lateral alignment (to within tens of microns) to the parabolic mirror that chiefly determine the vertical divergence of the BEaTriX's X-ray beam. The exact alignment of the crystals mostly affects the beam intensity, rather than the beam divergence.

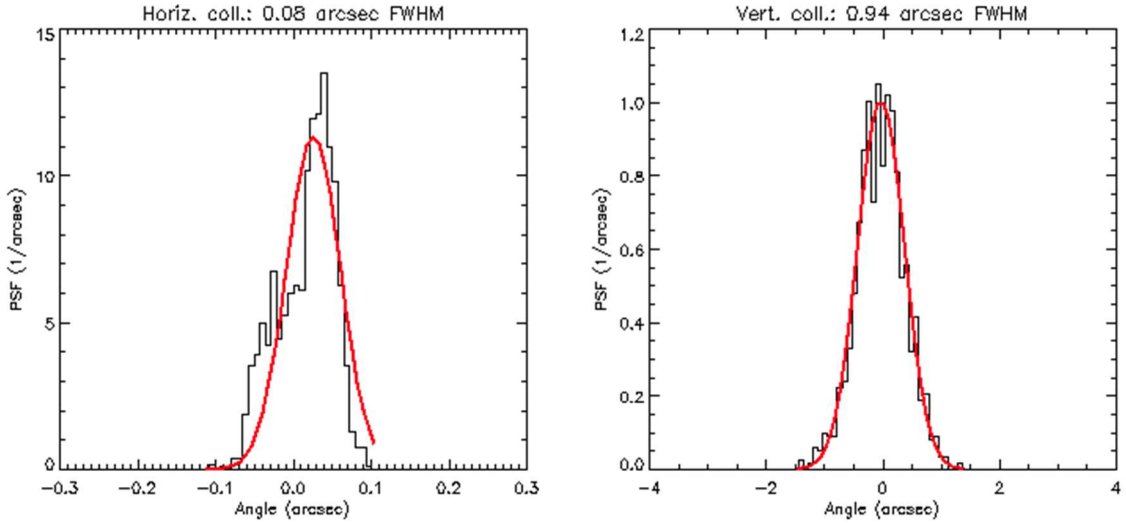

Fig. 5: achievable collimation of the BEaTriX system at 4.51 keV, in the horizontal and in the vertical direction, assuming components in their nominal position and a collimating mirror with a 3 arcsec HEW.

The dependence of the system performances as a function of the X–ray source size has been investigated. The baseline source is a Gaussian profile having a 30 µm FWHM in both (vertical and horizontal) directions in order to keep the vertical divergence within 2 arcsec FWHM. Any increase of the vertical spot size would cause the beam divergence to increase in proportion. In the horizontal direction, however, the angular spread is compressed by a factor of ~50, and so the horizontal size can be also increased without the risk to damage the horizontal beam parallelism. The beam intensity might in principle altered because the incidence angles on the monochromators would be spread and so might not always fulfill the Bragg condition. In reality, this does not occur, because an angular spread of even 10 arcsec corresponds to a broadening of the bandpass by just fractions of eV, which is on the order of the natural X-ray line width. For the same reason, the accuracy in the mirror profile (i.e. the focusing accuracy) does not need to be better than 10 arcsec HEW. The simulations shown in Fig. 6 prove that the system collimation remain within the specs if the horizontal source size increases up to a 500 µm FWHM.

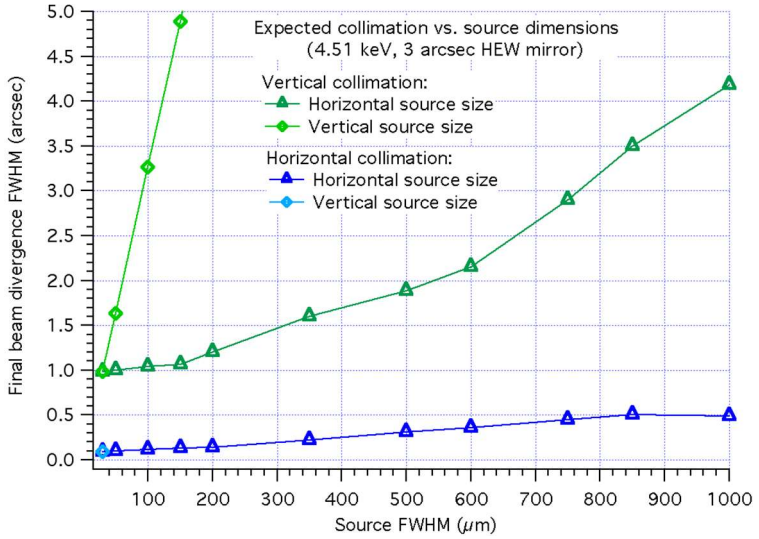

Fig. 6: performance variation in terms of beam collimation for increasing horizontal width of the X-ray source, assumed to be an ellipsoidal Gaussian profile with vertical FWHM of 30 µm.

Surprisingly, it is the vertical collimation that is affected by the horizontal source size: this is due to an increasing amount of coma aberration when parts of the source expand off-axis, and so the paraxial approximation is no longer fulfilled. The horizontal collimation is, as expected, partly restored by the asymmetric crystal properties. The flux is not significantly affected until the source size exceeds ~750 µm.

Fig. 7 reports the results of another series of simulations, in which the 30 µm x 30 µm source was displaced along the 3 axes, aiming at determining the mirror alignment tolerances. In all the cases considered, the horizontal divergence is almost unaffected because of the divergence compression operated by the asymmetric crystal. The vertical divergence does change, however. A few mm movement along the x-axis (Fig. 7 left, and refer to the reference frame shown in Fig. 2) causes a moderate defocusing, but almost no change is observed as long as the displacement from the best focal plane is within ± 1 mm. The other directions are more critical, however. For example (Fig. 7, right), the source cannot move along z by more than ± 200 µm before some collimation degradation starts to appear. This tolerance is stricter than along x, but it is still easy to fulfil with precision motors. The most sensitive direction is along y: an acceptable displacement might be ± 30 µm in order to remain below a vertical divergence of 1.25 arcsec. Beyond this limit, the beam divergence increases very rapidly. These displacement errors dictate for the mirror positioning repeatability (which clearly has to oversample the tolerance), the following values:

- In translation: 0.1 mm along x, 10 µm along y, and 50 µm along z.
- In rotation: 2 arcsec around y, 0.5 arcsec around z.

Other simulations aimed to determine analogous alignment tolerances for the other components (e.g., crystals) will be performed in the next months, using the same IDL code.

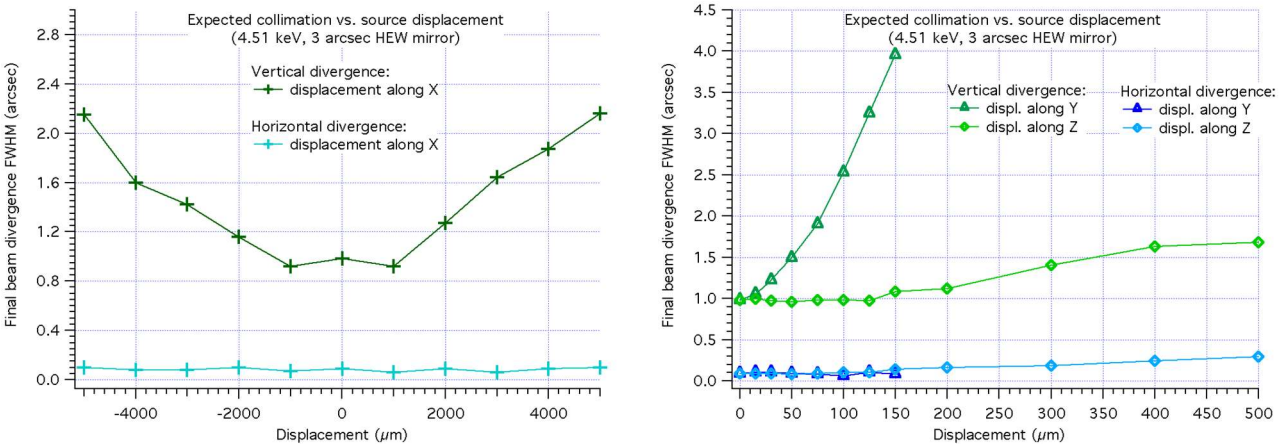

Fig. 7: performance variation in terms of beam collimation degradation for displacements X-ray source, with respect to the collimating mirror's focus. The source FWHM is fixed at 30 µm in both directions.

3. VACUUM SYSTEM DESIGN

We have completed a preliminary design of the vacuum system, including tubes and tanks to maintain the optical components of BEaTriX under low vacuum (10^{-2} mbar), in collaboration with the Vaqtec company (Torino, Italy). Viewed from outside (Fig. 8), BEaTriX is composed of two arms, made of vacuum tubes and chambers, roughly forming an "L" shape and enclosing the optical components sketched in Fig. 1. The corner corresponds to the asymmetric crystal, where the beam is approximately deviated by 90 deg in the horizontal plane. The short arm, approx. 6-m long and parallel to the laboratory basement, is responsible for the beam moderation (production, expansion and monochromation) and includes the source and the optical components. The long arm (~13 m) represents the optical bench that includes the MM handling stage, followed by a 12 m-long tube that propagates the X-ray focused by the MM to the focal plane, ending with a directly-illuminated CCD in fixed position. In order to follow the focused beam - that will be deviated downwards by the double reflection on the MM - the 12-m long tube shall be tilted in the vertical plane in a 0 - 7.2 deg range, corresponding, respectively, to the direct beam detection and the angular deviation by the largest radii of ATHENA. The short arm, in contrast, will be steered horizontally to adjust the angle between the two arms when the testing energy is changed, and so satisfy the Bragg law with either crystal. Some vacuum joints are flexible to enable the angle setting. All the pipeline will be mounted in a self-bearing structure, with the vacuum tubes counterbalanced with calibrated weight in order to minimize the motor load. The tubes are built modular (Fig. 9) to make intra-focal measurements, and possibly reduce the MM-CCD measurement distance, should the telescope focal length be reduced in the next future.

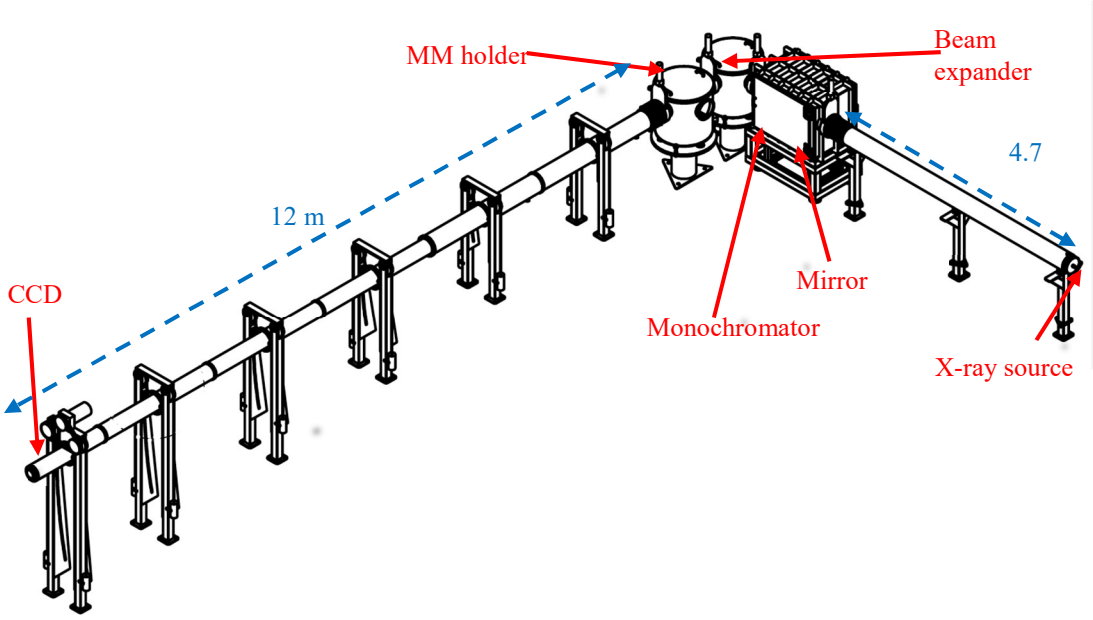

Fig. 8: outer layout, preliminary design of the BEaTriX facility. The optical elements needed to generate (X-ray source), filter, polarize and expand the beam (parabolic mirror, collimators, symmetric crystals, asymmetric crystal) are located in the "short arm" section. The 12 m vacuum tube (the "long arm") allows the ray to be focused on the detector. The short arm can be steered in the horizontal plane to fit the Bragg angle on the asymmetric crystal, while the long arm can be tilted vertically to fit the reflection angle of the MM under test. Vacuum pumps are not shown.

The laboratory where BEaTriX will be housed at INAF-OAB is actively being built at INAF-OAB (Sect. 5), and expected to be completed by April 2018. It is not designed as a clean room: however, using a heating/conditioning system, the room temperature will be maintained near 20 °C for proper operation of the instruments and convenience of the users. Considering the quite loose tolerance in the mirror-source distance (Sect. 2), there is no need to control the facility temperature to stricter limits than a few degrees (the temperature of the SPO MM under test will be controlled by the sample holder). A clean tent (ISO4 class or better), usually mounted above the sample holder tank, will allow us mounting/removing the MM under test without dust contaminations. The clean tent will be designed to be movable for being positioned above any other section that possibly needs to be opened (e.g., for inspection or maintenance of the optical components). Finally, in order to avoid the contamination of the tank with water vapor and dust, the sample chamber (or any other tube section) will be vented and purged with high-purity nitrogen.

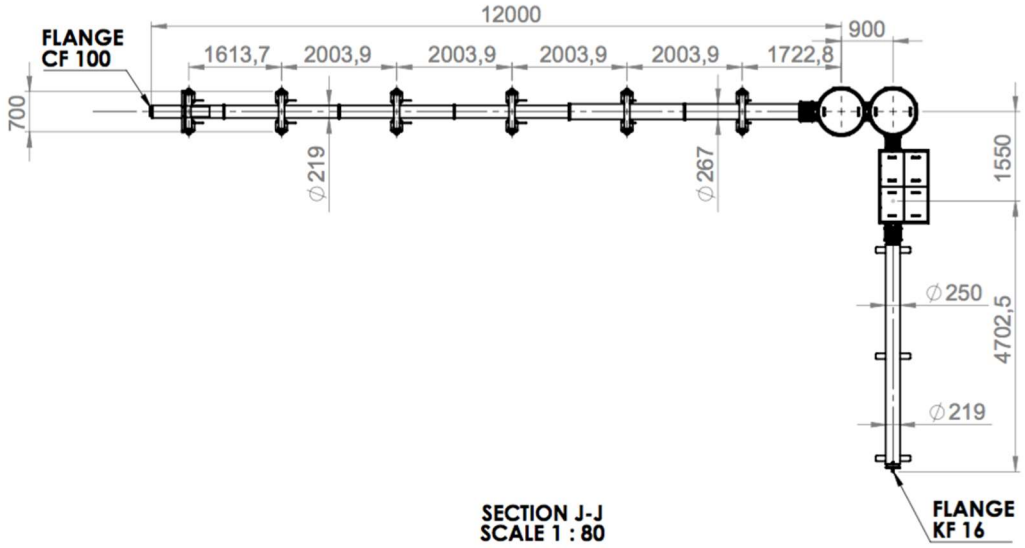

Fig. 9: the designed vacuum system, viewed from top. Vacuum pumps are not shown.

All the system needs to be evacuated to avoid X-ray absorption in air. The total range of X-rays from source to detector, at the end of the 12-m long tube, is approx. 19 m. The reduced dimensions of the facility

require only a moderate vacuum level: in a previous simulation[7] we had already shown that even a 0.1 mbar residual pressure would suffice to preserve 98% of the beam intensity at 4.51 keV. In order to allow us to use the system also at 1.49 keV, a vacuum level of 10^{-2} mbar of residual nitrogen in the vacuum tank should to be reached (transmissivity 97% at 1.49 keV). In this design, 6 scroll pumps can be used to independently evacuate the facility, divided into 6 vacuum section.

A flanged tube with approx. 200 mm diameter and a 4700-mm length connects the X-ray source to the collimating mirror chamber (Fig. 10). The X-ray source does not need to be enclosed in vacuum: it will be rather interfaced to the tube end via a fixed flange. The source will remain in air, injecting the X-rays directly in the vacuum. The 4700-mm tube connects the subsequent tank via a bellow in order to rotate it in the horizontal plane and adjust the incidence angle of the source on the crystal, and is evacuated via a dedicated pump.

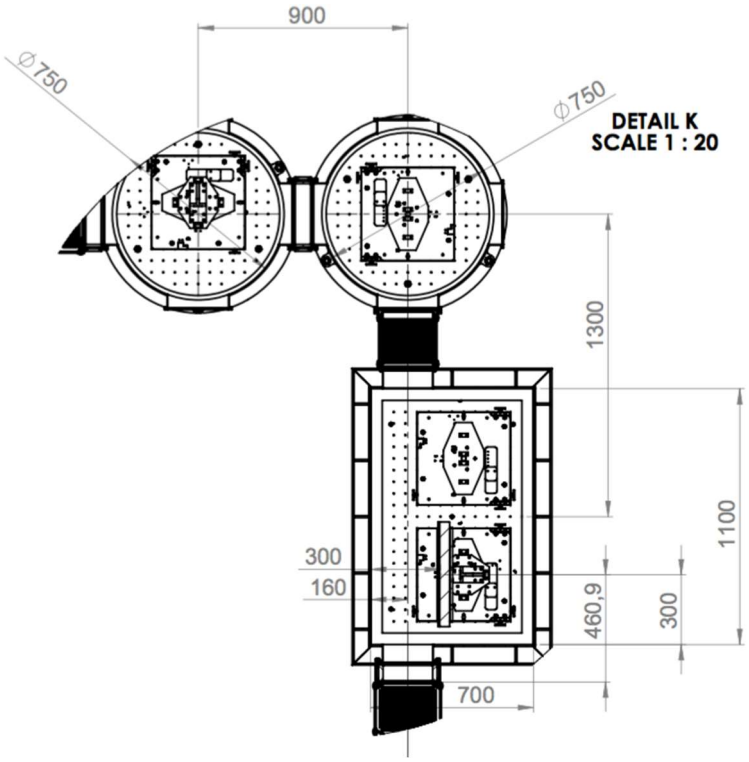

Fig. 10: detailed view (from top) of the vacuum chambers housing the parabolic mirror + the monochromation stage (the rectangular chamber), the beam expander and the MM holder (the cylindrical chambers).

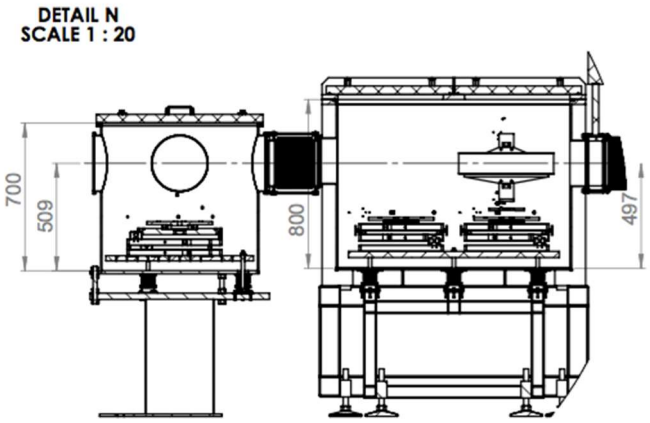

Fig. 11: sectional view of the vacuum chambers containing the parabolic mirror + monochromators (right) and the beam expander (left). A valve can be closed to isolate the 4750-mm tube on the right side from the vacuum tanks. All the optical components are mounted on precision motor stages. The motor stages are fixed to optical planes that are directly laid on the basement of the laboratory, in order to isolate the components from possible vibrations of the vacuum tanks connected to the pumps. Insulation from vibrations coming from the ground is ensured via dampers mounted on the legs.

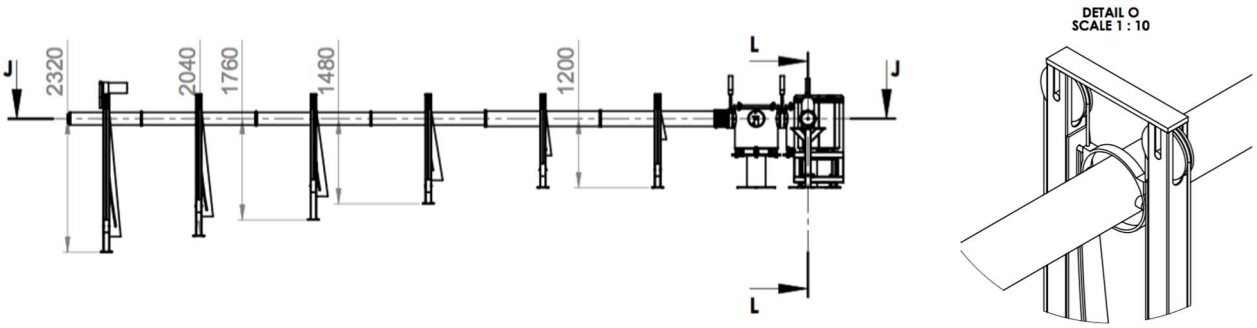

Fig. 12: (left) the 12-m long tube, seen sideways. We note the legs with different lengths in order to enable the up-down tilt of the tube and match the beam deviation downwards after reflection; (right) a detail of the counter-balancing system for the long tube.

Another chamber of length 1100 mm, and 700 mm width (Fig. 10 and Fig. 11), includes the mirror with its kinematic mount and the 3 translation and 3 rotation stages to accurately align the collimating mirror (Sect. 4.2). A lateral porthole is needed to possibly intervene in the alignment. This vacuum tank also includes the monochromator Channel Cut Crystal mounted on a lateral translation stage to align the monochromator into the beam. The stage mounts two CCC, one to filter the 1.49 keV (in ADP) and another to filter the 4.51 keV (in silicon) fluorescence line: the selection of either energy can be obtained translating either CCC into the beam. This section is equipped with vacuum valves on both ends, and a vacuum pump.

A tank with approx. 750 mm diameter (Fig. 10 and Fig. 11), connected to the previous tank via a circular flange, contains the asymmetric crystal (Sect. 4.1). The tank height is much higher than the crystal height (60 mm), not only in order to leave room for the motors that will align the crystal, but also to mount more than one crystal type (asymmetric silicon for the 4.51 keV setup, ADP for the 1.49 keV setup) and select the one that matches the energy required. This tank ends with a vacuum valve and is equipped with a vacuum pump.

The next chamber, of diam. 750 mm (Fig. 10 and Fig. 11), encloses the MM under test and the motors that enable alignments in 6 degrees of freedom and off-axis measurements. A lateral porthole is needed for sample removal/mounting. This section is equipped with vacuum valves on both ends and an independent vacuum pump, in order to vent/evacuate only this section when the sample is changed.

A 12-m long tube, 20 cm diam., finally allows the X-rays to propagate to focus after reflection on the module under test. The tube consists of separated joints, connected to each other via vacuum flanges. All the tube has to be supported by an isostatic mount and tilted in the vertical plane to follow the beam reflected downwards by the SPO MM (Fig. 12). The maximum tilt should be 1.5 m over the 12-m length. In contrast, the minimum tilt should be zero in order to measure the intensity of the direct beam prior to the MM exposure and so measure the effective area. The tube is ended by the detector, a directly-illuminated CCD with photon counting capabilities and high spatial resolution. The distance of the focal plane to the sample can be adjusted in two ways: moving the MM under test along the beam (a 10-cm total travel) for the fine focus search, and moving the detector along the long tube axis for a coarse focus search (in a range TBD). This is made possible by a flexible vacuum joint (a bellow) that will be used to move the focal plane without placing all the detector in vacuum. Efficient evacuation of this section is ensured by two vacuum pumps.

4. COMPONENT MANUFACTURING AND TESTING

4.1. The beam expanding silicon crystal (procured)

An asymmetrically-cut crystal (i.e., with diffraction planes tilted with respect to the surface[10]) is the component that expands the monochromatic and collimated beam in the horizontal direction. In the 4.5 keV setup, the crystal is in silicon and has the (220) diffraction planes tilted by 44.7 deg with respect to the outer surface (Fig. 13). The beam, with an effective width of 4 mm, impinges in grazing incidence on the crystal surface, but the incidence angle is anyway larger than the critical incidence angle of silicon at 4.51 keV; hence, the total external reflection is minimized. The 60 mm x 4 mm beam is spread over the crystal surface and is reflected with respect to the tilted (220) planes. Because of the incidence angle close to 45 deg on the Bragg planes, the beam is reflected near a right angle off-surface, and the horizontal beam size is expanded by a factor of 50. The final beam has thereby the same size of the crystal face (60 mm x 200 mm), fulfilling the initial request, and can be used to fully illuminate the aperture of the MM under test.

This project is funded by the European Union

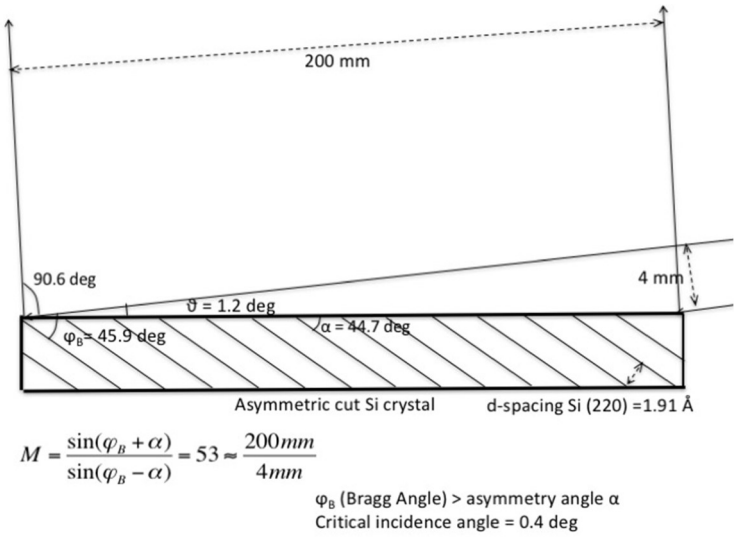

Fig. 13: principle of X-ray beam expansion via an asymmetrically-cut crystal. The incidence angle is larger than the critical incidence angle at 4.51 keV (0.4 deg) on silicon to avoid total external reflection. The real crystal has a 170 mm width, so the resulting beam will have a 170 mm width.

Fig. 14: the beam expanding crystal for the 4.51 keV setup, monocrystalline silicon, with the proper asymmetric cut at 44.7 deg from the (220) planes. The surface has been polished to remove the lattice damage introduced by the cut. The crystal dimensions are: 170 mm x 60 mm x 20 mm.

The silicon crystal with the correct asymmetric cut has been procured and tested. A high-purity silicon blank (from MEMC) has been cut and polished at IMEM-CNR (Parma, Italy). The crystal width has been reduced to 170 mm because of the maximum workable dimension allowed by the circular saw available at IMEM-CNR, but a 170 mm wide beam still remains in the specification (Sect. 1). Two crystals have been produced with the same cut; the crystal faces to be used to expand the beam had to be subsequently etched, to remove the surface damage introduced by the saw. The first crystal was polished using an abrasive slurry and was so made shiny (Fig. 14). The second was etched chemically and has an opaquer surface. The surface does not need to be polished to an optical level in reality, because the diffraction does not occur at the surface, but in the crystal bulk.

X-ray tests performed at 8.045 keV at IMEM-CNR (Fig. 15) using the (004) order. In fact, the (220) order cannot be explored at this X-ray energy, but the measurement of the 004 planes returns equivalent information about the correct orientation of the crystal cut with respect to the crystal lattice, and on the residual surface layer damage.

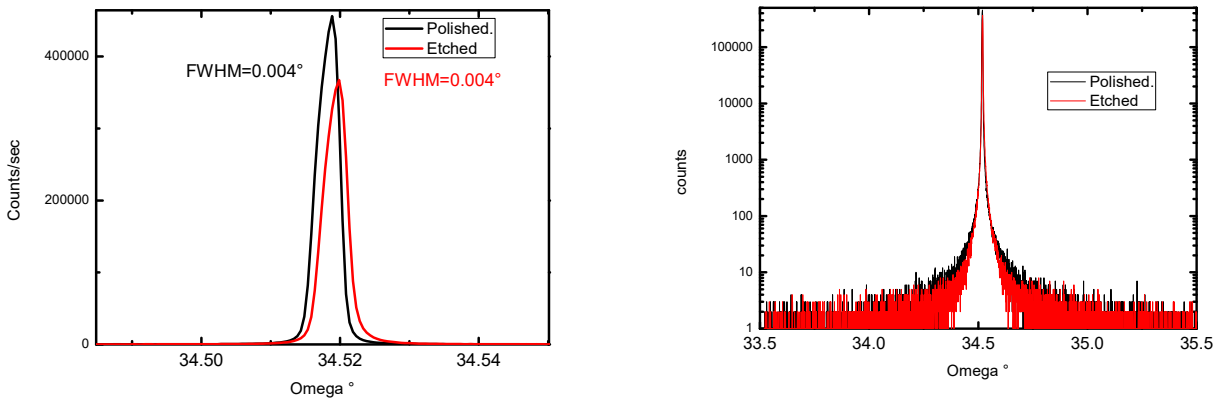

Fig. 15: measured diffraction peaks at 8 keV for the order (004) in the two procured asymmetric silicon crystals. The black diffraction curve refers to the polished crystal shown in Fig. 14. The etched crystal (red curve), which was etched chemically, exhibits a lower reflectivity. Left: linear scale. Right: log scale.

The (004) diffraction peaks have the same FWHM of the impinging X-ray beam (12 arcsec) used for the test. The two crystals have similar quality and comparable with the quality of a perfect crystal. Also, the asymmetry angle was measured repeating the measurements after rotating the crystal by 180 deg around the normal and subtracting the peak angles. As a result, the (001) planes form a 0.408 deg angle with respect to the outer surface: this means that the (220) planes form an angle of 45 deg - 0.408 deg = 44.592 deg with the surface, in excellent agreement with the 44.7 deg nominal value for the asymmetry angle (Fig. 13). Using this value, the expansion factor for the 220 diffraction at the Bragg angle 45.9 deg becomes:

$$\mathrm{b} = \frac{\sin(\vartheta_B + \varphi)}{\sin(\vartheta_B - \varphi)} = \frac{\sin(45.90 + 44.59)}{\sin(45.90 - 44.59)} = 43.7$$

which would expand the initial 4 mm-wide beam to a 175 mm size. As the crystal is 170 mm-wide, all the crystal width is well exploited and the resulting 170 mm width even exceeds the 120 mm required (Sect. 1). Additional tests, in a quasi-parallel beam, are foreseen at PANTER at the nominal wavelength of 4.51 keV.

For the 1.49 keV setup, silicon cannot be used because the d-spacing is too small and X-rays would not be diffracted. It has to be replaced by a crystal with larger d-spacing and lower absorption coefficient such as ADP (101) - Ammonium Dihydrogen Phosphate, $NH_4H_2PO_4$ (5.32 Å d-spacing, corresponding to a 50.85 deg Bragg angle). This crystal is still to be procured, but we have already found a company (Saint-Gobain) that can provide us ADP crystals having the appropriate characteristics.

4.2. Collimating mirror and related metrology (work in progress)

A paraboloidal, grazing incidence mirror with a 4.75 m focal length (measured from the side nearest to the source) and a 6 cm-high illuminated surface is necessary to make the beam parallel and pre-expand the beam in the vertical direction to a 6 cm size. The X-ray source is located just in the focus of the paraboloid within the tolerances listed in Sect. 2. The mirror will be coated with a platinum layer (30 nm) and an amorphous carbon overcoating (3 nm) to enhance the low-energy reflectivity. Forming a grazing incidence angle of 0.9 deg, the mirror exhibits high reflectivity up to the cut-off energy at 6.5 keV.

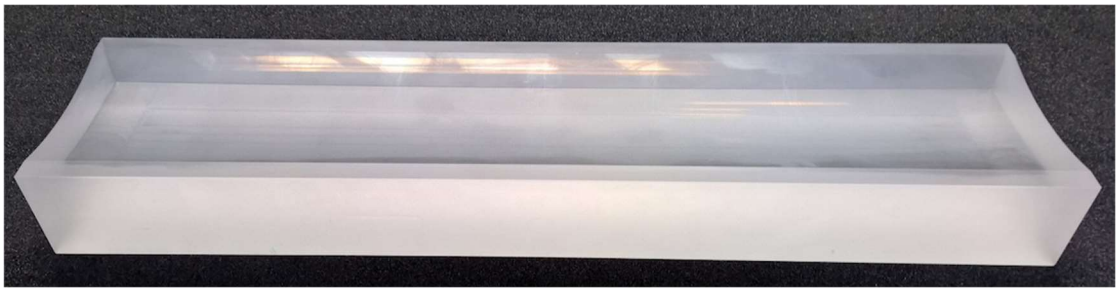

Fig. 16: one of the two paraboloidal mirrors procured from Carl Zeiss SMT GmbH, after the preliminary grinding. The mirror was subsequently lapped to partially smooth the periodic pattern left after grinding.

The paraboloidal mirror, with a 4750 mm focal length, a 153.5 mm curvature radius on the side near the source, a 436 mm length and a 60 mm aperture, has already been purchased from Zeiss in a preliminary grinding/pre-polishing stage (Fig. 16). The surface quality has been measured by Zeiss and is – as expected - by far too rough for the mirror to be used (HEW = 60 arcsec of figure accuracy, not to count the roughness). In order to work properly in BEaTriX, we need to improve the mirror accuracy down to a HEW ≈ 3 arcsec, otherwise the beam angular spread will exceed the monochromator angular region of high-reflectivity. At INAF-OAB, we have all the facilities to perform a polishing to this level: a deterministic polishing Zeeko machine and an Ion Beam Figuring for nanometric finishing of the surface relief.[11] Before proceeding to any polishing run, however, we need to perform an accurate and repeatable metrology of the surface: with the support of the Media-Lario company, we will use the MPR[12] metrologic machine (Fig. 17, left), able to return a consistent picture of the topography of a pseudo-cylindrical surface with this size and curvature to a few nanometers level. We have manufactured a support tool to interface the MPR to the paraboloidal mirror, and preliminary measurements show a very promising agreement with the measurements provided by Zeiss (Fig. 17, right). Measurements foreseen in the next months will return a 2D mapping of the surface and provide a reliable input to the Zeeko polishing tool and to the IBF process at INAF-OAB.

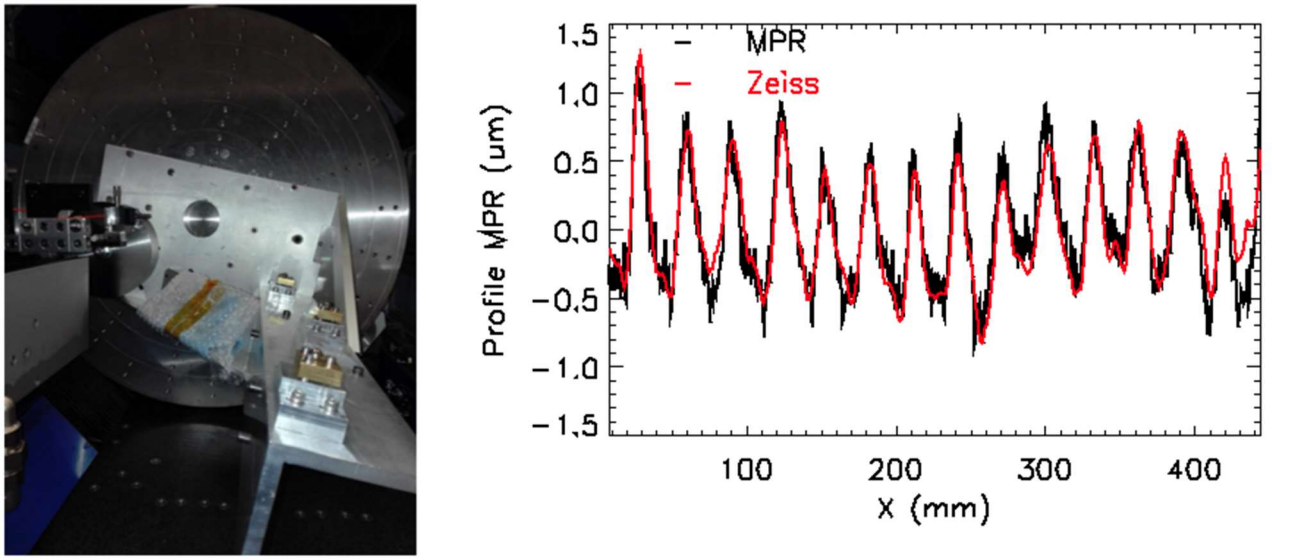

Fig. 17: (left) the MPR (Mandrel-Profile-Rotondimeter) installed at Media-Lario srl, equipped with the supporting sytem used to bear the parabolic mirror for a metrological characterization. Right: longitudinal profiles of the parabolic mirror, as purchased in the preliminary grinding/polishing status, measured with the MPR and by the manufacturer (Zeiss). The periodic pattern, residual of the initial grinding, needs to be removed at INAF-OAB by polishing and Ion Beam Figuring.

4.3. The X-ray source (to be procured soon)

A microfocus X-ray source with either aluminum (1.49 keV setup) or titanium (4.51 keV setup) anode will be used to generate an intense X-ray beam including the fluorescence lines and a bremsstrahlung continuum: the electron spot source has to be extremely small (30 µm x 30 µm) to ensure the required vertical collimation. Microfocus sources of this kind the available on the market: we have identified a specific model from Incoatec (Germany) that in addition generate a copious X-ray flux (on the order of 10^{12} ph/s/cm^2). The model with titanium anode can be already procured, while the source with aluminum anode is more difficult to operate because it can easily melt down. We are currently oriented toward the purchase of a *hybrid* X-ray source, with anode in Al-Ti alloy, able to generate the two Kα fluorescence lines at the same time. Selection of either line is operated simply moving either monochromator (in silicon or ADP) and the respective asymmetric crystal (in silicon or ADP). We have already received from Incoatec a quotation for a hybrid source, along with simulations (Fig. 18) of its expected spectrum. Both Kα are generated together: moreover, varying the accelerating voltage it is possible to modify the intensity ratio between the two lines, privileging either line for each setup. This approach has the additional advantage that the X-ray source does not need to be changed every time the X-ray setup changes from low-to high-energy and vice versa; this also means that the source position will be known very precisely and the component alignment will be extremely repeatable and easy to reproduce, when shifting from an energy to the other.

This project is funded by the European Union

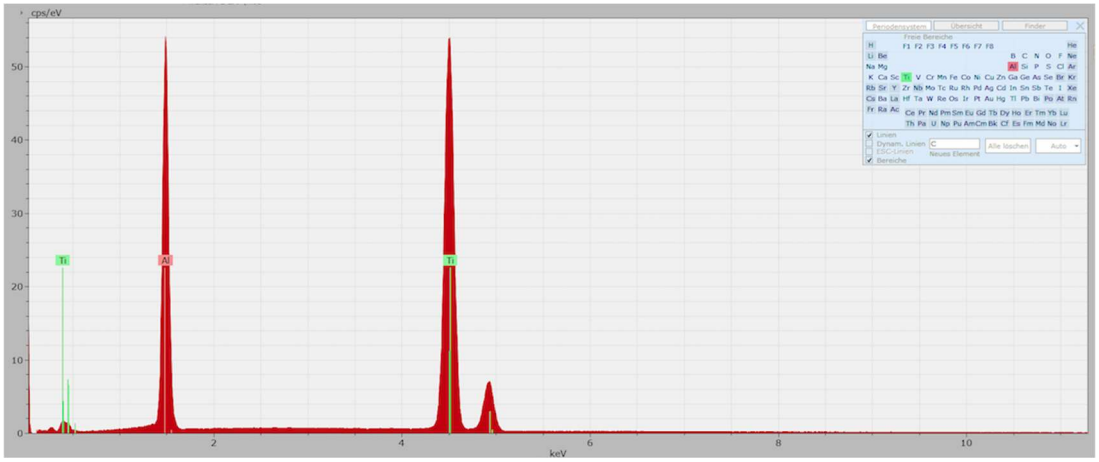

Fig. 18: simulated spectrum of a hybrid X-ray microfocus source with the anode in Ti-Al alloy (50% Al and 50% Ti). We clearly notice the presence of the X-ray fluorescence lines of both elements. In this simulation, the anodic voltage is 25 kV: changing the voltage allows one to vary the aluminium-to-titanium line intensity ratio (courtesy by Incoatec, reported with permission).

5. LABORATORY DESIGN AND ADVANCEMENT

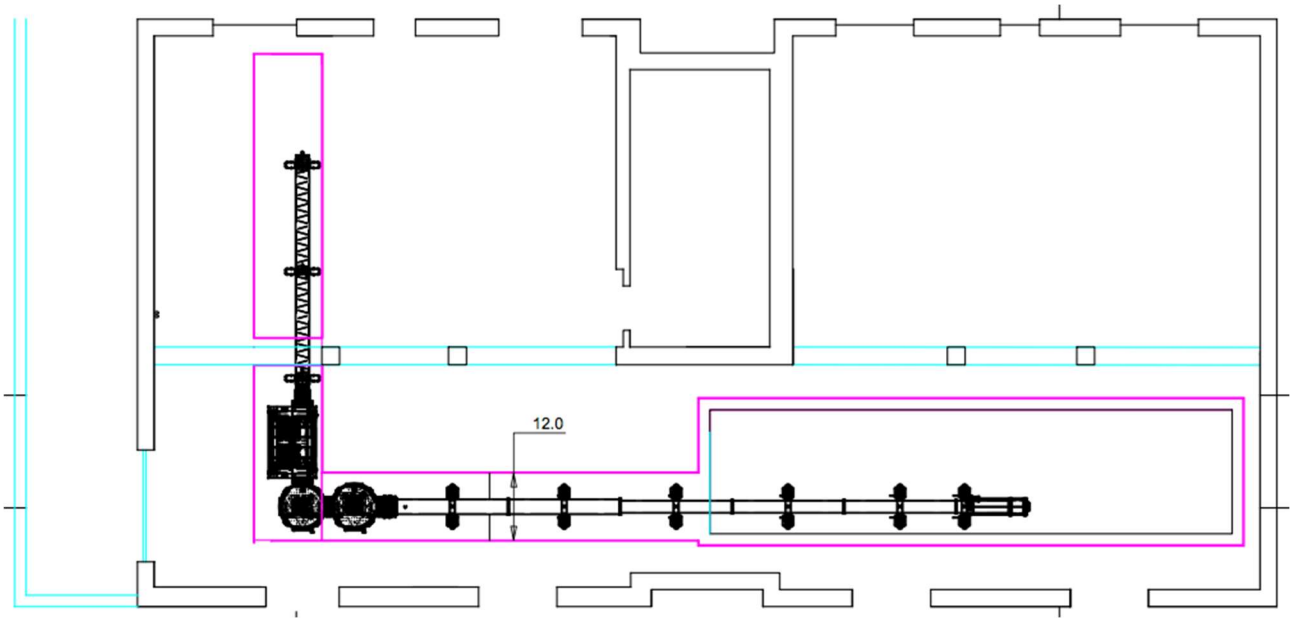

Fig. 19: a schematic project of the laboratory, in the building basement (formerly, the building cellars). The purple line delimits the concrete floor onto which BEaTriX will be built. The vacuum system project (Sect. 3) has been superimposed.

Finally, the works in the laboratory that will house BEaTriX are also going ahead. The laboratory does not require a large space because the facility is quite compact, but needs to be based directly on ground in order to limit the floor oscillations. It also has to be a closed and non-utilized space; therefore, we have chosen the cellars of a former house for researchers at INAF-OAB. Since all the apartments have now been turned to labs, also the underground floor can be converted to a laboratory. After removing all the non-structural walls, a schematic plan of the lab with the project of BEaTriX superposed is shown in Fig. 19. There will be, in the end, even much more room than needed.

A very important point that has been studied regards the minimization of vibrations coming from the ground and that can propagate to the facility: since the source has to remain in the focus within a 40 μm lateral distance, and the detector camera cannot move more than 1 pixel (15 μm) laterally (wrt the SPO MM under test), the floor has to properly designed. To this end, we have performed measurements of ground vibration and MASW (Multichannel Analysis of Surface Waves), finding that the ground is affected by

vibrations in the micron range only when operators walk around, otherwise vibrations have a nanometric amplitude and so are completely negligible for the present scopes.

The portion of the laboratory over which BEaTriX will be installed (purple line in Fig. 19) will be a solid concrete block, laid on a mattress of special rubber (Isolmant damp®) and isolated from the rest of the floor by a small gap. Its large mass and separation from the rest of the lab will avoid the transmission of vibrations to the optical components. Moreover, as we will need to tilt the long arm up and down by 1.5 m approx., a "trench" will be left in the concrete block, near the detector. A detailed lab design is shown in Fig. 20 and Fig. 21. The final design of the basement has to be confirmed by a Finite Element Analysis aimed at determine the amount of vibrations effectively transmitted to the facility. Anyway, the renovation works of the laboratory are already in progress and should be completed by April 2018. The design of the vacuum system will be finalized soon after that time, and we will continue with the procurement of the BEaTriX parts.

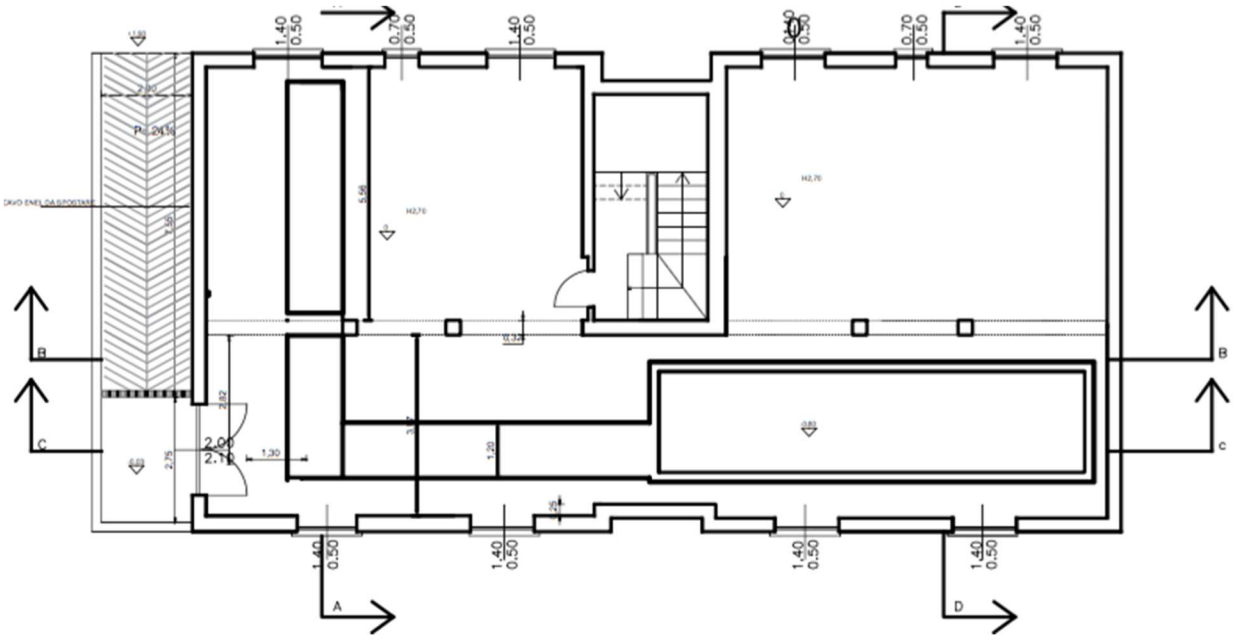

Fig. 20: detailed plan of the new laboratory that will house BEaTriX. An external ramp (on the left side) will be built to allow us an easy access to the lab from outside and introduce the vacuum components.

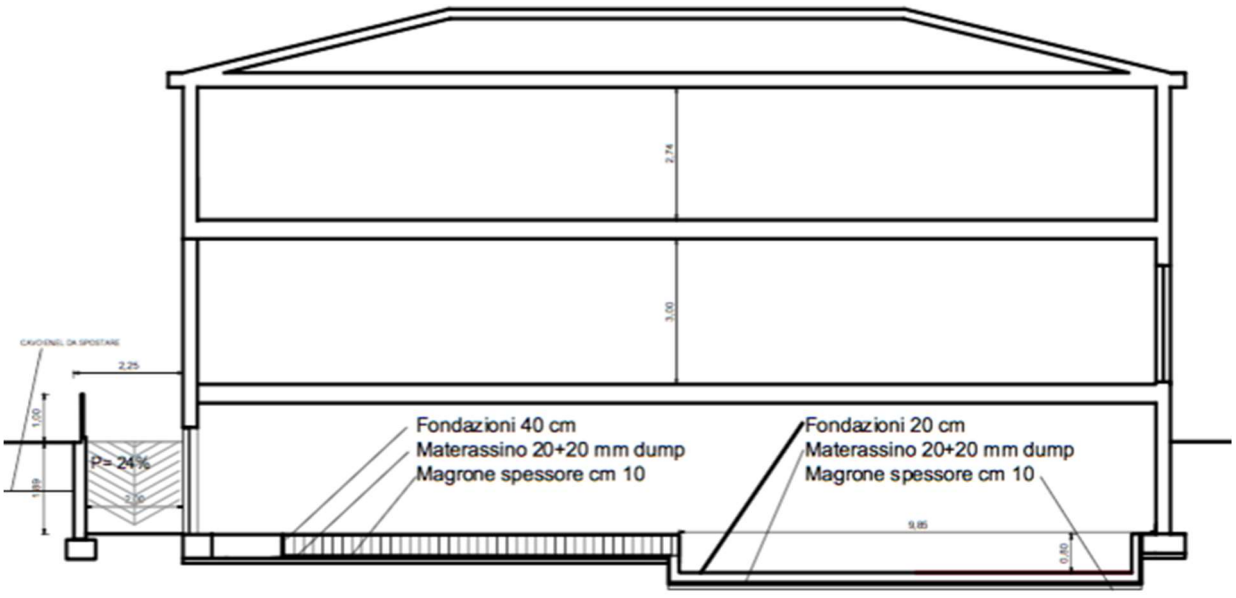

Fig. 21: sectional view of the new laboratory that will house BEaTriX: all the facility will be mounted on a heavy concrete basement laid on a damping rubber layer to avoid the propagation of vibrations from the ground to the optical elements.

REFERENCES

[1] Burwitz, V., Bavdaz, M., Pareschi, G., et al., "In focus measurements of IXO type optics using the new PANTER x-ray test facility extension," Proc. SPIE 8861, 88611J (2013)
[2] Bavdaz, M., Wille, E., Shortt, B., et al., "The ATHENA optics development," Proc. SPIE 9905, 990525 (2016)
[3] Bavdaz, M., Wille, E., Ayre, M., et al., "The Athena telescope and optics status," Proc. SPIE 10399, 103990B (2017)
[4] Collon, M.J., Vacanti, G., Günther, R., et al., "Silicon pore optics for the ATHENA telescope," Proc. SPIE 9905, 990528 (2016)
[5] Spiga, D., Christensen, F., Bavdaz, M., et al., "Simulation and modeling of silicon pore optics for the ATHENA X-ray telescope," Proc. SPIE 9905, 99055O (2016)
[6] Spiga, D., Della Monica Ferreira, D., Shortt, B., et al., "Optical simulations for design, alignment, and performance prediction of silicon pore optics for the ATHENA x-ray telescope," SPIE Proc. 10399, 103990H (2017)
[7] Spiga, D., Pareschi, G., Pelliciari, C., et al., "Functional tests of modular elements of segmented optics for x-ray telescopes via an expanded beam facility," Proc. SPIE 8443, 84435F (2012)
[8] Pelliciari, C., Spiga, D., Bonnini, E., et al., "BEaTriX, expanded soft x-ray beam facility for test of focusing optics, an update," Proc. SPIE 9603, 96031P (2015)
[9] Spiga, D., Pelliciari, C., Salmaso, B., et al., "Design and advancement status of the Beam Expander Testing X-ray facility (BEaTriX)," Proc. SPIE 9963, 996304 (2016)
[10] Christensen, F., Hornstrup, A., Frederiksen, P., et al., "Expanded beam x-ray optics calibration facility at the Daresbury Synchrotron," Proc. SPIE 2011, 540 (1994)
[11] Ghigo, M., Basso, S., Civitani, M., et al., "Ion beam figuring of large prototype mirror segments for the EELT," Proc. SPIE 9151, 91510Q (2014)
[12] Sironi, G., Citterio, O., Pareschi, G., et al., "MPR: innovative 3D free-form optics profilometer," Proc. SPIE 8147, 814718 (2011)